Journal of Luminescence 247 (2022) 118848

Contents lists available at ScienceDirect

Journal of Luminescence

journal homepage: www.elsevier.com/locate/jlumin

Full Length Article

The kinetic parameters of the main thermoluminescence glow peak of Al_2O_3:C,Mg: A critical evaluation of different analytical methods

J.M. Munoz [a], E.M. Yoshimura [b], M.L. Chithambo [c], L.G. Jacobsohn [d], N.M. Trindade [a,b,*]

[a] Department of Physics, Federal Institute of Education, Science and Technology of São Paulo, São Paulo, SP, Brazil
[b] Institute of Physics, University of São Paulo - USP, São Paulo, SP, Brazil
[c] Department of Physics and Electronics, Rhodes University, PO Box 94, Grahamstown, 6140, South Africa
[d] Department of Materials Science and Engineering, Clemson University, Clemson, SC, USA

ARTICLE INFO

Keywords:
Al_2O_3:C,Mg
Thermoluminescence
Radiation dosimetry
Computational analysis

ABSTRACT

Carbon and magnesium co-doped aluminum oxide (Al_2O_3:C,Mg) is a highly sensitive luminescence dosimeter with promising use in a wide spectrum of radiation-related applications, including neutron dosimetry and as a fluorescent nuclear track detector (FNTD). The goal of this work is to critically evaluate diverse methods and approaches for the determination of the kinetic parameters using Al_2O_3:C, Mg as a case study. Al_2O_3:C, Mg was beta irradiated with doses from 0.1 to 0.6 Gy. Besides thermoluminescence (TL) peaks at 325, 350, and 375 K, the analysis of the activation energy, frequency factor and order of kinetics focused exclusively on the main TL peak at 450 K. Analysis by curve fittings used a number of freeware, namely, *Glowfit*, *TLAnal*, the Thermoluminescence Glow Curve Deconvolution (TGCD) package, and the spreadsheet TLDecoxcel. The results from the computational approaches were compared with results obtained by analyzing experimental data using conventional methods as initial-rise, whole glow peak, variable heating rate and peak shape. The performance of the computational methods is satisfactory as the values found are consistent with the ones determined by the methods listed above.

1. Introduction

Al_2O_3:C, Mg is a high sensitivity luminescent material [1–3]. Recent studies point to its use as a potential dosimeter of beta particle [3], neutrons [4], protons and other charged particles [5], X-rays [6], gamma rays [7], as well as ultraviolet radiation [8,9].

The synthesis of Al_2O_3:C, Mg crystals by the Czochralski method in a highly reducing atmosphere promotes the formation of oxygen vacancies [10,11]. Additionally, the presence of C and doping by Mg facilitates the formation of oxygen vacancies that become F-type centers when filled by electrons [12]. Aggregated and perturbed F-type centers (F^+(Mg), F^{2+}(Mg), F_2^{2+}(Mg), F^+(2 Mg), F^{2+}(2 Mg), F_2^{2+}(2 Mg)) also occur. The increase in the concentration of F and F^+ centers, as well as the formation of F-aggregate centers, enhances the luminescence response [5] positively affecting the material as a sensor for ionizing radiation.

Thermoluminescence (TL) has a long history of successful applications, particularly in personal dosimetry [13]. TL appears in irradiated semiconductors and insulators upon heating, and suitable dosimeters are the ones whose TL intensity is proportional to the absorbed radiation dose [14]. The heating acts as a stimulus to free trapped electrons and the TL signal is generated upon the recombination of the free electron with a hole at the luminescence (recombination) center. Electrons trapped at different traps will be released at different temperatures corresponding to peaks in the TL temperature-resolved curve known as glow curve [14,15].

The TL glow curve shows one or more peaks, each corresponding to the emptying of trapped electrons from a type of trap [15,16]. From the analysis of these peaks, it is possible to obtain the kinetic parameters related to the TL mechanism in the material [17]. These parameters include the activation energy (E) associated with the trap, the frequency factor (s) associated with the vibration frequency of the crystalline structure, and the kinetic order (b) of the glow peak [18].

The most used methods for the analysis of the TL kinetic parameters are the peak shape, initial rise, whole glow peak, and variable heating rate [15,17,19]. In addition to that, since the 1980s, several methods of computational TL fitting have been developed to help in the processing of data. Many of the software contributions to glow curve deconvolution

* Corresponding author. Department of Physics, Federal Institute of Education, Science and Technology of São Paulo, São Paulo, SP, Brazil.
E-mail address: ntrindade@ifsp.edu.br (N.M. Trindade).

https://doi.org/10.1016/j.jlumin.2022.118848
Received 9 February 2022; Received in revised form 17 March 2022; Accepted 20 March 2022
Available online 23 March 2022

came from the GLOCANIN (Glow Curve Analysis Intercomparison) project [20]. Ever since, several freeware for the deconvolution of glow curves have been developed taking advantage of different TL models [20–25]. Among the different functions and programs developed, *Glowfit*, *TLAnal* and Thermoluminescence Glow Curve Deconvolution (TGCD) are frequently used [17,24,26,27]. In addition, the TLDecoxcel spreadsheet is a newly developed interface that is also available as open source [28].

Although Al_2O_3:C, Mg is a promising material that has been widely investigated since the early 2000's, only limited effort to characterize its response by means of dedicated computational methods for the analysis of TL kinetics has been carried out. In view of this, the main goal of this work is to determine the kinetic parameters of the main TL glow peak of Al_2O_3:C, Mg using computational methods and critically evaluate them against results obtained by conventional methods. In this regard, well-established methods have been used to determine the kinetic parameters of Al_2O_3:C, Mg in Refs. [8,29], as well as in this work.

2. Materials and methods

2.1. Sample and TL readout

A single crystal sample of Al_2O_3:C, Mg (Landauer Crystal Growth Division, USA) produced by the Czochralski method [12] was used. The sample was cut in the shape of a rectangular parallelepiped of dimensions $8 \times 1.6 \times 0.5$ mm^3 with one polished side, and mass of 48 mg.

The material was exposed to beta radiation from a $^{90}Sr/^{90}Y$ source (10 mGy/s) at room temperature, with total dose ranging from 0.1 to 0.6 Gy. Irradiation and TL measurements were executed with a TL/OSL Risø DA-20 reader. Luminescence was detected through a detection filter Hoya U-340 (thickness of 7.5 mm; transmission window within 290–370 nm) and a 5 mm diameter light collimator placed in front of a Hamamatsu H7421-40 photomultiplier tube. After each irradiation exposure, the material was heated (0.2–5 K/s, with 1 K/s being the standard heating rate unless noted otherwise) from 273 K to 573 K, and after each readout, a second TL (5 K/s) reading was performed to obtain the background signal. All measurements were carried out in nitrogen atmosphere to prevent spurious signals.

2.2. Kinetic parameters

The TL phenomenon can be described in terms of the rate of electrons being released from trapping centers. In the theoretical model developed by Randall and Wilkins [30], the escape probability rate of an electron from a trap (p) is given by the following expression:

$$p = s \exp\left(-\frac{E}{\mathrm{kT}}\right) \tag{1}$$

with,

$$s = \nu\kappa \ \exp\left(\frac{\Delta S}{\mathrm{k}}\right) \tag{2}$$

where E (eV) is the activation energy or trap depth, k is Boltzmann's constant ($k = 8.617 \times 10^{-5}$ eV/K), T is the absolute temperature (K), and s is the frequency factor (s^{-1}). The factor s corresponds to the frequency that the trapped electron interacts with the structure of the crystal (ν) multiplied by the probabilities of transition (κ) and by a term that associates the variation of entropy (ΔS) and Boltzmann's constant to the transition of electrons from traps to the conduction band [31], as indicated in eq. (2). In principle, the frequency factor denotes the number of times per second that a trapped electron attempts to detach from its binding potential [32].

In the simplest case, when the probability of electrons being re-trapped after release from a trap is very small when compared to the probability of recombining at the recombination centers, the TL mechanism is referred to as first-order kinetics. On the other hand, it is considered second-order kinetics when the probability of electrons being re-trapped is equal to or larger than the probability of electrons recombining in recombination centers [14].

The TL intensity I as a function of the temperature T for glow peaks that follow first-order kinetics is given by eq. (3):

$$I(T) = n_0 s \ \exp\left(-\frac{E}{kT}\right)\exp\left[-\frac{s}{\beta}\int_{T_0}^{T}\exp\left(-\frac{E}{kT}\right)\mathrm{d}T\right] \tag{3}$$

where n_0 is the initial concentration of trapped charges at T_0 corresponding to the irradiation temperature and β is the heating rate. In the case of second-order kinetics, considering a linear heating rate and a concentration of electron traps N, TL intensity can be obtained according to eq. (4) [33]:

$$I(T) = n_0^2 \frac{s}{N}\exp\left(-\frac{E}{kT}\right)\left[1 + \frac{n_0}{N}\int_{T_0}^{T}\frac{s}{\beta}\exp\left(-\frac{E}{kT}\right)dT\right]^{-2} \tag{4}$$

TL intensity for a general order kinetics b, where b is the order of the kinetics mechanism, is given by (eq. (5) [15]):

$$I(T) = \frac{n_0 s}{N} n_0^{(b-1)}\exp\left(-\frac{E}{kT}\right)\left[1 + \left(\frac{(b-1)n_0^{b-1}}{N}\right)\int_{T_0}^{T}\frac{s}{\beta}\exp\left(-\frac{E}{kT}\right)dT\right]^{b/(b-1)} \tag{5}$$

To determine the kinetic parameters of Al_2O_3:C, Mg exposed to beta radiation, different methods presented in the literature were used. Methods based on software packages to be discussed will be referred to as computational methods whereas established methods from the literature will be called conventional methods.

2.3. Glow curve computational methods

2.3.1. GlowFit

Introduced in 2003 [34], the *GlowFit* program performs fitting of TL curves based on the first-order kinetics model, considering the TL curve described according to eq. (6):

$$I(T) = I_M \exp\left(\frac{E}{kT_M} - \frac{E}{kT}\right)\exp\left\{\frac{E}{kT_M}\left[\alpha\left(\frac{E}{kT_M}\right) - \frac{T}{T_M}\exp\left(\frac{E}{kT_M} - \frac{E}{kT}\right)\alpha\left(\frac{E}{kT}\right)\right]\right\} \tag{6}$$

where I_M and T_M are the maximum intensity and its associated temperature of the TL peak, and $\alpha(x)$ is a function with constants values generated by the program. It is described according to eq. (7):

$$\alpha(x) = 1 - \frac{a_0 + a_1 x + a_2 x^2 + a_3 x^3 + x^4}{b_0 + b_1 x + b_2 x^2 + b_3 x^3 + x^4} \tag{7}$$

The fittings are executed according to the Levenberg-Marquardt algorithm [35].

2.3.2. TLAnal

The best fit procedure with the *TLAnal* program is based on the general kinetics order model [36,37]. This is referred to as the General Approximation (GA) model and its main assumptions are that the free carrier concentration in the conduction band and its rate of change are much smaller than the trapped carrier concentration and its rate of change respectively. In the fitting, two minimization methods are used, the Hessian and the simplex methods, towards the optimizing of computing time [38].

2.3.3. TGCD

The TGCD package is based on the functions developed by Kitis and collaborators [39,40]. Based on the investigation of the three functions

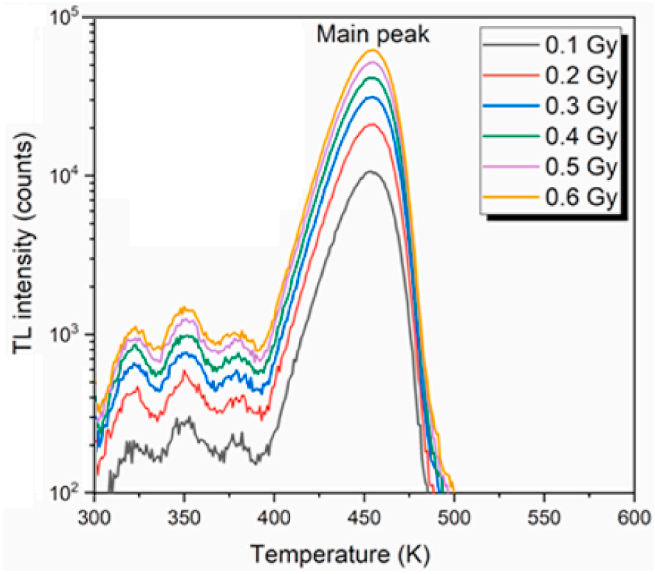

Fig. 1. TL response of Al_2O_3:C, Mg exposed from 0.1 to 0.6 Gy of beta radiation.

present in the package, the adjustments that best fit the data set correspond to the glow curve intensity described by g_1 algorithm used in the package, presented in eq. (8).

$$I(T) = I_M b^{b/b-1} \upsilon \left[(b-1)\left(1 - \frac{2kT}{E}\right) \frac{T^2}{T_M^2}\upsilon + Z_m \right]^{-\frac{b}{b-1}} \quad (8)$$

where $\upsilon = exp\left(\frac{E}{kT}\frac{T-T_M}{T_M}\right)$, $Z_m = 1 + \frac{2kT_M(b-1)}{E}$

The value of s is determined based on eq. (9) [39].

$$s = \frac{\beta E}{kT_M^2}\frac{1}{Z_M} exp\left(\frac{E}{kT_M}\right) \quad (9)$$

The package also uses the Levenberg-Marquardt algorithm for best fitting.

2.3.4. TLDecoxcel

The TLDecoxcel algorithm is designed for use in Microsoft Excel application spreadsheets [28]. The program performs glow curve fitting assuming a general order kinetics that is described by the equations proposed for the OTOR ('one trap, one recombination center') model [39]. In practice, the values of the kinetic parameters are determined based on estimates of the free parameters maximum intensity and temperature of the glow peak, kinetic order and activation energy proposed by the user considering the figure of merit (FOM) value. Various

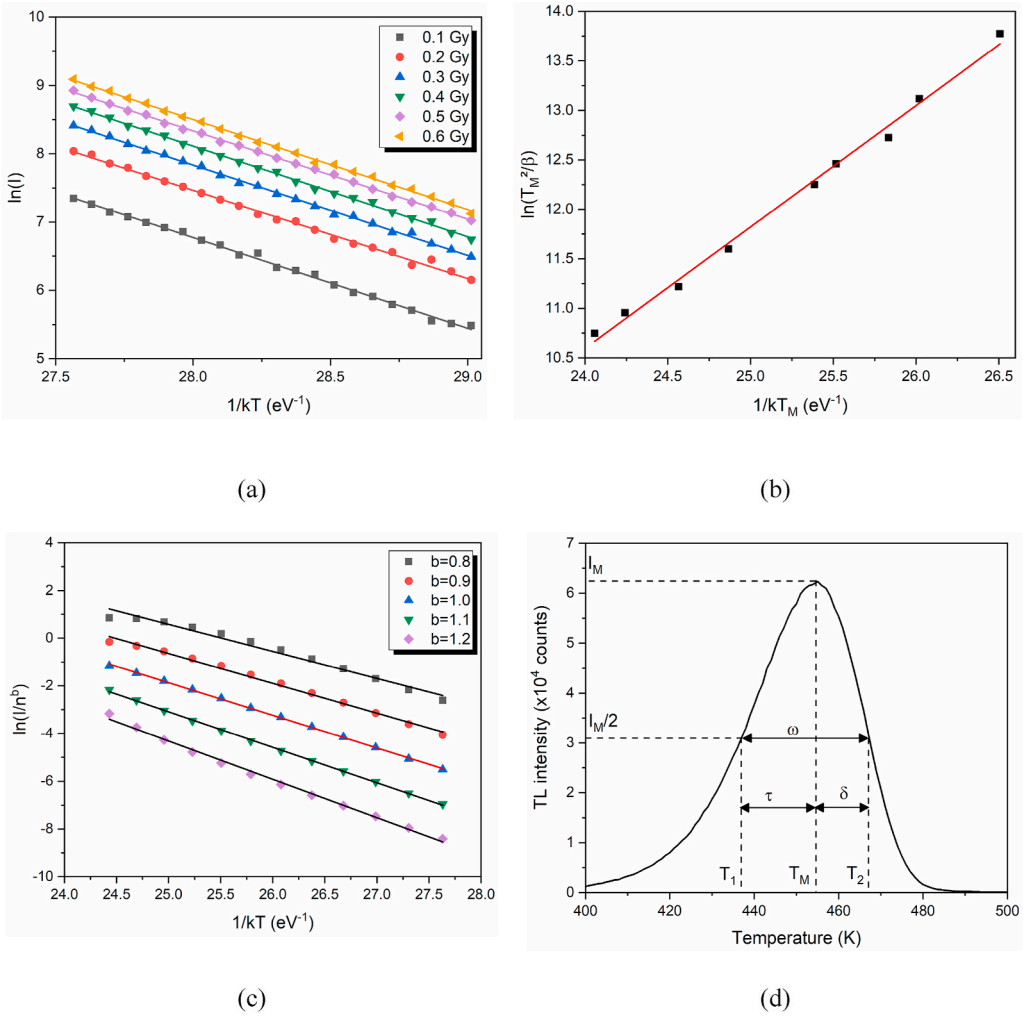

Fig. 2. Analysis of experimental results using the methods of (a) initial rise for doses from 0.1 to 0.6 Gy, (b) variable heating rate for heating rates from 0.2 to 5 K/s and a dose of 0.1 Gy, (c) whole glow peak for dose of 0.6 Gy with kinetic order testing from 0.8 to 1.2, and (d) peak shape for dose of 0.6 Gy, where T_1 and T_2 are the temperatures associated to the glow-peak semi-widths at half of the maximum intensity.

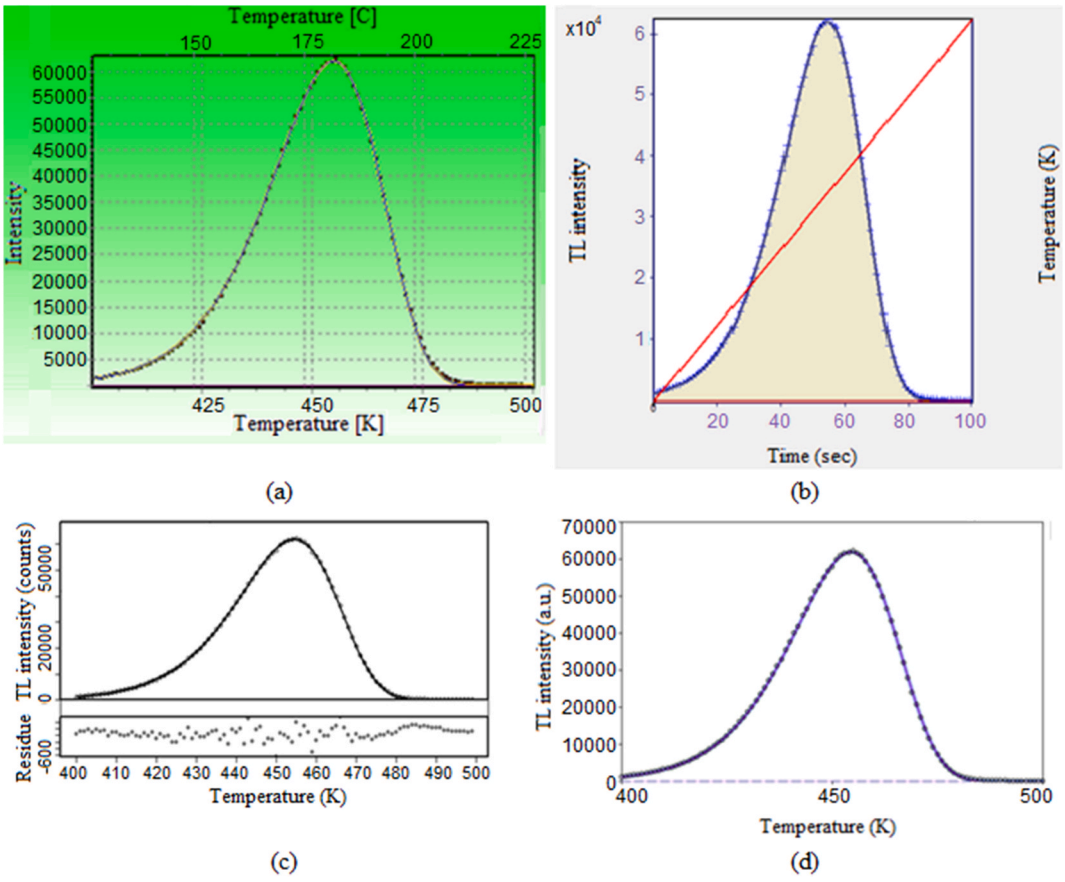

Fig. 3. Fitted curves of the main TL peak of Al_2O_3:C, Mg irradiated with 0.6 Gy of beta radiation by (a) *GlowFit*, (b) *TLAnal*, (c) TGCD, and (d) TLDecoxcel. In (b), the red line corresponds to the temporal evolution of the temperature. In (c) the residues are shown at the bottom.

interactions may be needed to obtain acceptable FOM values. With the use of the "Solver" add-on [41], the process is facilitated and the kinetic parameters are determined based on the nonlinear Generalized Reduced Gradient (GRG) algorithm [42,43].

3. Results and discussion

The TL glow curves obtained from Al_2O_3:C, Mg previously exposed to beta radiation for different irradiation doses from 0.1 to 0.6 Gy are presented in Fig. 1. These glow curves serve to illustrate the well-known response of this material to radiation. The glow curves are dominated by emission near 450 K (the main TL peak), in addition to other low intensity (about two orders of magnitude lower) peaks at lower temperatures (~325 K, ~350 K and ~375 K). In this work, as mentioned earlier, we focused on the main TL peak that is responsible for the dosimetric functionality of the material. RL measurements of Al_2O_3:C, Mg shows that the emission of main TL peak is resultant of emissions from several F-type centers at 325 nm (F^+), 415 nm (F), 520 nm (F_2^{2+}(2 Mg)) and 750 nm (F^{2+} (2 Mg)) [44,45]. It was also possible to observe in Fig. 1 a linear increase of the intensity of the main TL glow peak with the increase of the radiation dose, giving rise to the already known linear dose response of this material [8]. Furthermore, no shift of the main TL peak was observed with increasing radiation dose demonstrating the first order kinetics of its TL mechanism.

The TL kinetic parameters of Al_2O_3:C, Mg exposed to beta radiation were obtained with the initial rise, variable heating rate, whole glow peak and peak shape methods. Representative plots related to these methods are presented in Fig. 2 a, b, c and d, respectively. In addition, the fitted glow curves obtained directly by the computational methods *GlowFit*, *TLAnal*, TGCD and TLDecoxcel, are illustrated in Fig. 3 a, b, c and d, respectively, for a beta irradiation dose of 0.6 Gy.

In this work, the kinetic parameters E, s and b of the main glow peak were obtained for each and all irradiation doses using all computational methods previously discussed. For each method, the average of each kinetic parameter taken over all irradiation doses is presented in Table 1. Also, the FOM for all fittings was evaluated by the respective programs according to eq. (10) [34,39]:

$$FOM[\%] = \frac{\sum_i |y_i - y(x_i)|}{\sum_i y_i} \times 100\% \quad (10)$$

where y_i are experimental values, and $y(x_i)$ the corresponding fitted values. In order to compare the quality of the computational fittings, the fitting result with the best (smallest) FOM was selected for presentation in Table 1.

The analysis of the results focused first on the value of the activation energy E, according to the conventional and computational methods, as summarized in Table 1, followed by the analysis of the frequency factor s. The comparison of the conventional results of E between this work and the literature showed the values of E to be within the 1.23–1.37 eV range ($\Delta E = 0.14$ eV). The IR and the VHR methods had the highest discrepancy, 0.12 eV and 0.08 eV, respectively, with the results obtained in this work being systematically lower than those from Ref. [29]. These discrepancies, of about 0.1 eV, were beyond the expected uncertainties though below 10% of the E values. The global average of all conventional results, including this work and [29], yielded the value $E = 1.33$ eV with a standard deviation of 0.05 eV. This value was used as a reference for the analysis of the computational results.

All computational methods achieved excellent FOM values, with *GlowFit* being slightly higher than the other methods. The computational E values were within the much narrower 1.36–1.411 eV range ($\Delta E =$

Table 1
Kinetic parameters of the main TL glow peak ($T_M \sim 450$K) of Al_2O_3:C, Mg exposed to beta radiation from 0.1 to 0.6 Gy obtained in this work by different methods, in addition to the values extracted from the literature that are presented in the last three columns.

Methods	This work				Literature		
	E (eV)	s (s^{-1})	b	Best FOM (%)	E (eV)	s (s^{-1})	b
IR	1.24 ± 0.02	–	–	–	1.36 ± 0.01 [29]	–	–
VHR	1.23 ± 0.03	$(2.2 \pm 1.9) \times 10^{12}$	1	–	1.31 ± 0.02 [29]	(1.18×10^{14}) [29]	–
WGP	1.36 ± 0.01	$(8.4 \pm 3.3) \times 10^{13}$	1	–	1.37 ± 0.01 [29]	(7.72×10^{14}) [29]	1 [29]
Peak shape (τ)	1.36 ± 0.01	–	1	–	1.36 ± 0.13 [29]	–	1 [29]
Peak shape (δ)	1.30 ± 0.01	–			1.35 ± 0.24 [29]	–	
Peak shape (ω)	1.35 ± 0.01	–			1.37 ± 0.12 [29]	–	
Glowfit	1.38 ± 0.01	$(1.63 \pm 0.03) \times 10^{14}$	1	1.22	1.37 ± 0.01 [8]	–	1 [8]
TLAnal	1.411 ± 0.003	$(3.5 \pm 0.3) \times 10^{14}$	1	0.73	–	–	–
TGCD	1.411 ± 0.001	$(3.51 \pm 0.09) \times 10^{14}$	1	0.72	1.36 ± 0.01 [29]	–	–
TLDecoxcel	1.39 ± 0.01	–	1	0.73	–	–	–

0.051 eV, nearly 3x narrower than the conventional range), with the TGCD method yielding the largest discrepancy of 0.051 eV. This discrepancy was, nevertheless, less than 4% of the average E value. The *TLAnal* and TGCD methods yielded the largest difference in relation to the average E value, 0.081 eV, that was about 6% of the average E value. Interestingly, all computational methods yielded values (in most cases slightly) higher than the average conventional E value. However, taking into consideration the respective uncertainties, *Glowfit* and TLDecoxcel methods yielded values within the standard deviation of the average E value, while *TLAnal* and TGCD methods values did not. The average of all computational results, including this work [8,29], yielded the value $E = 1.39$ eV with a standard deviation of 0.02 eV. We also conclude that the computational E was 4.5% higher than the conventional E, however, it is noted that they agree within their standard deviations. The global average energy value of all conventional and computational results was 1.35 eV with a standard deviation of 0.05 eV.

The analysis of s obtained from conventional results, both in this work and in Ref. [29], showed a very large discrepancy, from 0.0217×10^{14} s^{-1} to 7.72×10^{14} s^{-1}, that is of about 3 orders of magnitude. On the other hand, the s values obtained from computational methods yielded a much narrower range, within 1.63×10^{14} s^{-1} to 3.51×10^{14} s^{-1}. These values are in reasonable agreement with the ones obtained from conventional results as reported in Ref. [29]. Based on an average value of the frequency factor obtained from the computational methods (2.57×10^{14} s^{-1}) and global average energy value ($E = 1.35$ eV), as well as assuming first-order kinetics and a room storage temperature (295K), the lifetime (τ) can be estimated by eq. (11) [31]:

$$\tau = s^{-1} \exp\left(\frac{E}{kT}\right) \quad (11)$$

which gives approximately ~ 20.5 years, that is, a fairly stable TL glow peak.

4. Conclusions

An investigation of the kinetic parameters of the main TL glow peak of Al_2O_3:C, Mg exposed to beta radiation was carried out using different conventional methods such as initial rise, whole glow peak, variable heating rate and peak shape. In addition to that, the computational method using programs such as *GlowFit*, *TLAnal*, TGCD, and TLDecoxcel was also used. Overall, the results for E were found from 1.23 eV to 1.37 eV, while the average of all conventional results yielded $E = 1.33 \pm 0.05$ eV and the average of all computational results yielded $E = 1.39 \pm 0.02$ eV. The E values obtained by computational methods tended to be slightly higher than the ones obtained by conventional methods, though they agree within their standard deviations. The global average energy value of all conventional and computational results was 1.35 ± 0.05 eV. In terms of s, a large discrepancy spanning several orders of magnitude was found. The results obtained by computational methods were in a much narrower range than those obtained by conventional methods.

Credit author statement

J. M. Munoz: Investigation, Formal analysis, Data curation, Writing – original draft. E. M. Yoshimura: Resources, Supervision, Writing-Review&Editing. M. L. Chithambo: Supervision, Writing-Review&Editing. L. G. Jacobsohn: Supervision, Writing-Review&Editing. N. M. Trindade: Conceptualization, Methodology, Validation, Writing – original draft, Writing-Review&Editing.

Declaration of competing interest

The authors declare that they have no known competing financial interests or personal relationships that could have appeared to influence the work reported in this paper.

Acknowledgments

J.M. Munoz (#2019/22375–2) and N.M. Trindade (#2019/05915–3, #2018/05982–0) thank the São Paulo Research Foundation (FAPESP). E.M. Yoshimura is grateful to the National Council for Scientific and Technological Development (CNPq), #306843/2018–8, and FAPESP, #2018/05982–0. This material is based upon work supported by the National Science Foundation under grant no. 1653016 to Clemson University. The authors are grateful to Dr. M.S. Akselrod from Landauer, Inc., Crystal Growth Division, Stillwater, OK, for the α-Al_2O_3:C,Mg crystal.

References

[1] M.L. Chithambo, J.M. Kalita, A.A. Finch, F- and F^+-band radioluminescence and the influence of annealing on its emission spectra in Al_2O_3:C,Mg, Radiat. Meas. 134 (2020) 106306, https://doi.org/10.1016/j.radmeas.2020.106306.
[2] J.M. Kalita, M.L. Chithambo, The effect of pre-dose on thermally and optically stimulated luminescence from α-Al_2O_3:C,Mg and Al_2O_3:C, Appl. Radiat. Isot. 140 (2018) 69–75, https://doi.org/10.1016/j.apradiso.2018.06.012.
[3] J.M. Kalita, M.L. Chithambo, The effect of annealing and beta irradiation on thermoluminescence spectra of α-Al_2O_3:C,Mg, J. Lumin. 196 (2018) 195–200, https://doi.org/10.1016/j.jlumin.2017.12.036.
[4] G.J. Sykora, M.S. Akselrod, Photoluminescence study of photochromically and radiochromically transformed Al_2O_3:C,Mg crystals used for fluorescent nuclear track detectors, Radiat. Meas. 45 (2010) 631–634, https://doi.org/10.1016/j.radmeas.2009.11.022.
[5] M.S. Akselrod, G.J. Sykora, Fluorescent nuclear track detector technology – a new way to do passive solid state dosimetry, Radiat. Meas. 46 (2011) 1671–1679, https://doi.org/10.1016/j.radmeas.2011.06.018.
[6] G.J. Sykora, Photo- and Radiochromic Transformations in Al_2O_3:C,Mg Fluorescent Nuclear Track Detectors and High Resolution Imaging of Radiation Fields, Oklahoma State University, 2010.
[7] N.S. Saharin, H. Wagiran, A.R. Tamuri, Thermoluminescence (TL) properties of Al_2O_3: C, Mg exposed to cobalt-60 gamma radiation doses, Radiat. Meas. 70 (2014) 11–14, https://doi.org/10.1016/j.radmeas.2014.08.012.
[8] N.M. Trindade, M.G. Magalhães, M.C.S. Nunes, E.M. Yoshimura, L.G. Jacobsohn, Thermoluminescence of UV-irradiated α-Al_2O_3:C,Mg, J. Lumin. 223 (2020) 117195, https://doi.org/10.1016/j.jlumin.2020.117195.
[9] J.M. Munoz, L.S. Lima, E.M. Yoshimura, L.G. Jacobsohn, N.M. Trindade, OSL response of α-Al_2O_3:C,Mg exposed to beta and UVC radiation: a comparative

investigation, J. Lumin. 236 (2021) 118058, https://doi.org/10.1016/j.jlumin.2021.118058.
[10] C.D. Brandle, Czochralski growth of oxides, J. Cryst. Growth 264 (2004) 593–604, https://doi.org/10.1016/j.jcrysgro.2003.12.044.
[11] M.S. Akselrod, A.E. Akselrod, S.S. Orlov, S. Sanyal, T.H. Underwood, New aluminum oxide single crystals for volumetric optical data storage, Opt. Data Storage. 13 (2003), https://doi.org/10.1364/ODS.2003.TuC3. TuC3.
[12] M. Akselrod, J. Kouwenberg, Fluorescent nuclear track detectors – review of past, present and future of the technology, Radiat. Meas. 117 (2018) 35–51, https://doi.org/10.1016/j.radmeas.2018.07.005.
[13] S. Souza, T. Yamamoto, F. D'errico, Estado da arte em dosimetria do estado solido, in: Int. Jt. Conf. RADIO 2014, Gramado, 2014.
[14] E.G. Yukihara, S.W.S. McKeever, Optically Stimulated Luminescence: Fundamentals and Applications, UK, John Wiley and Sons, West Sussex, 2011.
[15] S.W.S. McKeever, Thermoluminescence of Solids, Cambridge University Press, Cambridge, 1985.
[16] R. Chen, V. Pagonis, Thermally and Optically Stimulated Luminescence: A Simulation Approach, John Wiley & Sons, West Sussex, 2011.
[17] P.P. Kulkarni, K.H. Gavhane, M.S. Bhadane, V.N. Bhoraskar, S.S. Dahiwale, S. D. Dhole, Investigation of the photoluminescence and novel thermoluminescence dosimetric properties of $NaGdF_4:Tb^{3+}$ phosphors, Mater. Adv. 1 (2020) 1113–1124, https://doi.org/10.1039/D0MA00247J.
[18] R. Chen, S.W.S. McKeever, Theory of Thermoluminescence and Related Phenomena, World Scientific, 1997, https://doi.org/10.1142/2781.
[19] V. Pagonis, G. Kitis, C. Furetta, Numerical and Practical Exercises in Thermoluminescence, first ed., Springer-Verlag, New York, 2006 https://doi.org/10.1007/0-387-30090-2.
[20] A.J.J. Bos, T.M. Piters, J.M. Gómez-Ros, A. Delgado, An Intercomparison of glow curve analysis computer programs: I. Synthetic glow curves, Radiat. Protect. Dosim. 47 (1993) 473–477, https://doi.org/10.1093/oxfordjournals.rpd.a081789.
[21] A.J.J. Bos, T.M. Piters, J.M. Gómez Ros, A. Delgado, An Intercomparison of glow curve analysis computer programs: II. Measured glow curves, Radiat. Protect. Dosim. 51 (1994) 257–264, https://doi.org/10.1093/oxfordjournals.rpd.a082143.
[22] J.F. Benavente, J.M. Gómez-Ros, A.M. Romero, Thermoluminescence glow curve deconvolution for discrete and continuous trap distributions, Appl. Radiat. Isot. 153 (2019) 108843, https://doi.org/10.1016/j.apradiso.2019.108843.
[23] M. El-Kinawy, H.F. El-Nashar, N. El-Faramawy, New handling of thermoluminescence glow curve deconvolution expressions for different kinetic orders based on OTOR model, in: J. Phys. Conf. Ser, Institute of Physics Publishing, 2019, p. 12012, https://doi.org/10.1088/1742-6596/1253/1/012012.
[24] J. Peng, G. Kitis, A.M. Sadek, E.C. Karsu Asal, Z. Li, Thermoluminescence glow-curve deconvolution using analytical expressions: a unified presentation, Appl. Radiat. Isot. 168 (2021) 109440, https://doi.org/10.1016/j.apradiso.2020.109440.
[25] L. Lovedy Singh, R.K. Gartia, Glow-curve deconvolution of thermoluminescence curves in the simplified OTOR equation using the hybrid genetic algorithm, Nucl. Instrum. Methods Phys. Res. Sect. B Beam Interact. Mater. Atoms 319 (2014) 39–43, https://doi.org/10.1016/j.nimb.2013.10.029.
[26] R.M. Baltezar, J.A. Nieto, Analysis of the BeO thermoluminescent glow curve by the deconvolution method, Appl. Radiat. Isot. 150 (2019) 53–56, https://doi.org/10.1016/j.apradiso.2019.04.003.
[27] S.W.S. McKeever, S. Sholom, Trap level spectroscopy of disordered materials using thermoluminescence: an application to aluminosilicate glass, J. Lumin. 234 (2021) 117950, https://doi.org/10.1016/j.jlumin.2021.117950.
[28] N.A. Kazakis, TLDECOXCEL: a dynamic excel spreadsheet for the computerised curve deconvolution of TL glow curves into discrete-energy and/or continuous-energy-distribution peaks, Radiat. Protect. Dosim. 187 (2019) 154–163, https://doi.org/10.1093/rpd/ncz150.
[29] J.M. Kalita, M.L. Chithambo, Thermoluminescence of α-Al_2O_3:C,Mg: kinetic analysis of the main glow peak, J. Lumin. 182 (2017) 177–182, https://doi.org/10.1016/j.jlumin.2016.10.031.
[30] J.T. Randall, M.H.F. Wilkins, Phosphorescence and electron traps - I. The study of trap distributions, Proc. R. Soc. London. Ser. A. Math. Phys. Sci. 184 (1945) 365, https://doi.org/10.1098/rspa.1945.0024.
[31] C. Furetta, Handbook of Thermoluminescence, World Scientific, 2003, https://doi.org/10.1142/5167.
[32] M.L. Chithambo, P. Niyonzima, J.M. Kalita, Phototransferred thermoluminescence of synthetic quartz: analysis of illumination-time response curves, J. Lumin. 198 (2018) 146–154, https://doi.org/10.1016/j.jlumin.2018.02.029.
[33] G.F.J. Garlick, A.F. Gibson, The electron trap mechanism of luminescence in sulphide and silicate phosphors, Proc. Phys. Soc. 60 (1948) 574, https://doi.org/10.1088/0959-5309/60/6/308.
[34] M. Puchalska, P. Bilski, GlowFit—a new tool for thermoluminescence glow-curve deconvolution, Radiat. Meas. 41 (2006) 659–664, https://doi.org/10.1016/j.radmeas.2006.03.008.
[35] J.J. Moré, The Levenberg-Marquardt algorithm: implementation and theory, Springer, Berlin, Heidelberg, 1978, pp. 105–116, https://doi.org/10.1007/bfb0067700.
[36] K.S. Chung, H.S. Choe, J.I. Lee, J.L. Kim, A new method for the numerical analysis of thermoluminescence glow curve, Radiat. Meas. 42 (2007) 731–734, https://doi.org/10.1016/j.radmeas.2007.02.028.
[37] C.M. Sunta, W.E.F. Ayta, R.N. Kulkarni, T.M. Piters, S. Watanabe, General-order kinetics of thermoluminescence and its physical meaning, J. Phys. D Appl. Phys. 30 (1997) 1234, https://doi.org/10.1088/0022-3727/30/8/013.
[38] K.S. Chung, H.S. Choe, J.I. Lee, J.L. Kim, S.Y. Chang, A computer program for the deconvolution of thermoluminescence glow curves, Radiat. Protect. Dosim. 115 (2005) 345–349, https://doi.org/10.1093/rpd/nci073.
[39] G. Kitis, J.M. Gomez-Ros, J.W.N. Tuyn, Thermoluminescence glow-curve deconvolution functions for first, second and general orders of kinetics, J. Phys. D Appl. Phys. 31 (1998) 2636–2641, https://doi.org/10.1088/0022-3727/31/19/037.
[40] A.M. Sadek, H.M. Eissa, A.M. Basha, E. Carinou, P. Askounis, G. Kitis, The deconvolution of thermoluminescence glow-curves using general expressions derived from the one trap-one recombination (OTOR) level model, Appl. Radiat. Isot. 95 (2015) 214–221, https://doi.org/10.1016/j.apradiso.2014.10.030.
[41] D. Fylstra, L. Lasdon, J. Watson, A. Waren, Design and use of the Microsoft excel solver, INFORMS J. Appl. Anal. 28 (1998) 29–55, https://doi.org/10.1287/inte.28.5.29.
[42] D. Afouxenidis, G.S. Polymeris, N.C. Tsirliganis, G. Kitis, Computerised curve deconvolution of TL/OSL curves using a popular spreadsheet program, Radiat. Protect. Dosim. 149 (2012) 363–370, https://doi.org/10.1093/rpd/ncr315.
[43] L.S. Lasdon, R.L. Fox, M.W. Ratner, Nonlinear optimization using the generalized reduced gradient method, Rev. Fr. Autom. Inf. Rech. Oper. 8 (1974) 73–103, https://doi.org/10.1051/ro/197408V300731.
[44] N.M. Trindade, L.G. Jacobsohn, Thermoluminescence and radioluminescence of α-Al_2O_3:C,Mg at high temperatures, J. Lumin. 204 (2018) 598–602, https://doi.org/10.1016/J.JLUMIN.2018.08.018.
[45] N.M. Trindade, L.G. Jacobsohn, E.M. Yoshimura, Correlation between thermoluminescence and optically stimulated luminescence of α-Al_2O_3:C,Mg, J. Lumin. 206 (2019) 298–301, https://doi.org/10.1016/j.jlumin.2018.10.084.